JOURNAL OF CATALYSIS 136, 141–148 (1992)

Simulation of Dynamic Behaviors of Simple Aromatic Hydrocarbons inside the Pores of a Pentasil Zeolite

YOSHIAKI NAKAZAKI,[1] NARUSHI GOTO,[2] AND TOMOYUKI INUI[3]

Department of Hydrocarbon Chemistry, Faculty of Engineering, Kyoto University, Sakyo-ku, Kyoto 606-01, Japan

Received January 3, 1990; revised November 21, 1991

Dynamic behaviors of benzene, toluene, and xylene isomers inside the pores of ZSM-5 were simulated using a super minicomputer. The results of calculations were visualized by means of computer graphics. Molecular diameters of these aromatic hydrocarbons are barely larger than the pore size of ZSM-5; however, from the calculation of molecular mechanics between these molecules and ZSM-5, it is clear that they are excited and can pass through the pores of ZSM-5. The energy level of *p*-xylene entering the pores of ZSM-5 with the methyl group in front was the lowest among the molecules studied in all positions of the pore channels. When these aromatics passed through the pores of ZSM-5, the interaction between the methyl groups of aromatics and the pore's wall of ZSM-5 was fairly large.

INTRODUCTION

A large number of investigations on characteristics of zeolites and their applications to catalytic reactions have been carried out. Separation and synthesis of many hydrocarbons are conducted in petroleum industries by applying the molecular shape selectivities of zeolites (*1*). However, the catalyst deactivation owing to the coke accumulations is always one of the most serious problems in those shape-selective zeolitic catalysts. Since the pore structure of a pentasil zeolite, ZSM-5, does not allow fused ring aromatic hydrocarbons to grow as coke precursors, much attention has been paid to this zeolitic catalyst.

Further progress has been made in the development of a number of metallosilicates catalysts in which the Al of ZSM-5 was replaced by other transition metals expecting intrinsic catalytic reaction characteristics. Especially, Ga-silicate (*2*) and Zn-silicate (*3*) exhibited excellent performances for aromatization of light paraffinic hydrocarbons. To improve the catalytic performance, quantitative understanding on the behaviors of aromatic hydrocarbon molecules is necessary.

In the previous study, the shape selectivity of zeolitic catalysts has often been explained qualitatively by comparison between the pore diameter of zeolites and the size of reactant molecules (*4*). However, quantitative studies on the dynamic behaviors of molecules inside pores of zeolites have not been made extensively.

Recently, Nowak *et al.* (*5*) and Mentzen and Bosselet (*6*) studied these subjects using computer simulations. Nowak *et al.* studied the influence of the framework geometry of zeolite on the adsorption and diffusion of benzene and toluene molecules inside theta-1 zeolite and silicalite by means of computer simulation. Mentzen and Bosselet described that some shape-selective and diffusion properties of MFI topology might be esti-

[1] Present address; Department of Applied Chemistry, Osaka Prefectural College of Technology, Neyagawa, Osaka 572, Japan.

[2] Present address; KUBOTA COMPUTER INC., Shinjuku-ku, Tokyo 160, Japan.

[3] To whom correspondence should be addressed.

0021-9517/92 $5.00

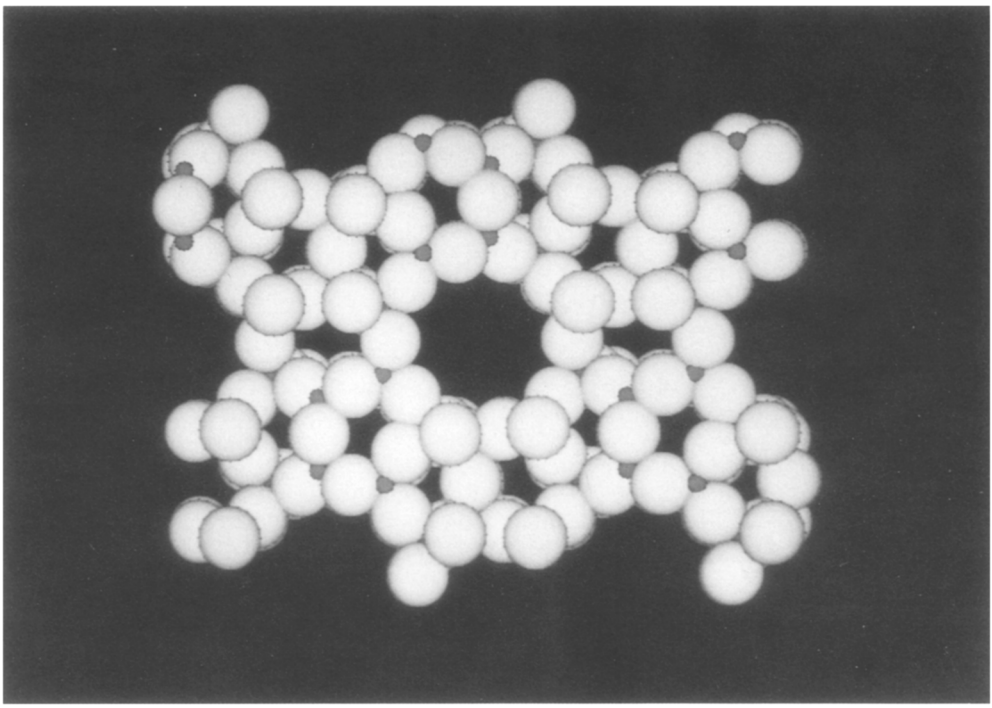

FIG. 1. Display of pore opening structure of ZSM-5 crystal by computer graphics.

mated theoretically by their computer simulations. However, in the former, their force field described only Lennard–Jones type interaction and molecular rotations. On the other hand, the latter studied interactions between aromatic hydrocarbons and zeolite using the Buckingham model. The former drew calculation results as contour lines of potential energy; it did not express how molecules were moving in practice. The latter drew merely the variation of the potential curve.

In our previous paper (*7*), the distinct differences between the behaviors of benzene and toluene molecules inside the pores of ZSM-5 were described by the potential energy calculation applying molecular mechanics.

In this paper, to more precisely study influences of the methyl groups between aromatic hydrocarbons and ZSM-5, the potential energies of xylene's isomers were calculated applying the Dreiding force field (*8, 9*). Calculation results were then visualized to understand the states of moving molecules.

METHOD

The interactions of atoms in a large system can be calculated using the theory of quantum mechanics. However, the amounts of calculation in this method would become astronomical. Therefore, practically, interactions between atoms should be described by empirical force fields based on classical mechanics.

The overall description of an N-body system in terms of a superposition of simpler terms is called a force field. Although the exact description must involve Schrödinger's equation for the electronic wave functions on each geometry, the accurate force fields are practically available for organic and biological systems and crystallography.

In the Dreiding force fields by Goddard and co-workers (*8, 9*), the potential energy, E, is expressed as a sum of bonded and nonbonded interactions, as

$$E = E_b + E_\theta + E_\phi + E_\omega + E_{vdw} + E_{el} + E_{hb}.$$

The bonded interactions consist of bond-stretching (E_b), bond-angle bending (E_θ), dihedral-angle torsion (E_ϕ), and inversion (E_ω) terms, while the nonbonded interactions consist of van der Waals (E_{vdw}), electrostatic (E_{el}), and hydrogen-bond (E_{hb}) terms.

In the Dreiding force field, the bond-stretching terms are of harmonic form:

$$E_{ij} = \tfrac{1}{2}k_{ij}(r - r_{ij})^2, \qquad (1a)$$

where k_{ij} is the force constant (in kJ · mol^{-1} · nm^{-2}) and r_{ij} is the standard or natural bond length (in nm). The natural bond length r_{ij} is assumed to be the sum of atomic radii for atom types i and j with a small correction:

$$r_{ij} = r_i + r_j - 0.01. \qquad (1b)$$

Atomic radii are obtained from structural data on standard reference compounds. The bond-stretching force constant k_{ij} is set to 4.189×10^7 kJ · mol^{-1} · nm^{-2} independent of i and j.

The angle-bending term in the Dreiding force field is of the conventional harmonic in theta form,

$$E_{ijk} = \tfrac{1}{2}K_{ijk}(\theta - \theta_{ijk})^2, \qquad (2)$$

where θ_{ijk} is the natural angle between the bonds ij and jk and K_{ijk} is in units of kJ · mol^{-1} · radian^{-2}. In the Dreiding force field, the bending-force constants are all assumed to be 419 kJ · mol^{-1} · radian^{-2}.

The torsional term for two bonds ij and kl connected via a common bond jk is chosen to be of the form

$$E_\phi = \tfrac{1}{2}V_\phi[1 + d \cdot \cos(n\phi\,\theta)]^2, \qquad (3)$$

where V_ϕ is one-half the rotational barrier in kilojoules per mole. n is the periodicity of the potential, and d (+1 or −1) is the phase factor.

For the Dreiding force field, the energy barriers are taken as one of three choices:

sp^2–sp^2 bonds or resonance central bonds: $V_\phi = 251$ kJ · mol^{-1}, $n = 2$, and $d = -1$.

sp^3 – sp^3 central bonds: $V_\phi = 12.6$ kJ · mol^{-1}, $n = 3$, and $d = +1$.

All other cases: $V_\phi = 1.3$ kJ · mol^{-1}.

For atoms i bonded exactly to three other atoms j, k, l, the inversion term is defined as if it were a torsion:

$$E_\omega = \tfrac{1}{2}k_\omega(\omega - \omega_0)^2. \qquad (4)$$

k_ω is the force constant (in kJ · mol^{-1} · radian^{-2}), and ω_0 is the natural improper torsion angle (the torsion angle of ij with respect to kl using the $j - k$ pseudobond) for planar system $\omega_0 = 0°$ and $k_\omega = 4187$ kJ · mol^{-1} · radian^{-2}; whereas for tetrahedral systems, $k_\omega = 167$ kJ · mol^{-1} radian^{-2} and $\omega_0 = 31.4°$. For cases where j or k are hydrogens, $\omega_0 = 35.2044°$.

Nonbonded interactions (van der Waals forces) are also included in the force field. A Lennard–Jones type expression is used,

$$E_{vdw} = D_{ij}\{-2[x_{ij}/x]^6 + [x_{ij}/x]^{12}\}, \qquad (5)$$

where D_{ij} is the well depth in kilojoules per mole and x_{ij} is the van der Walls bond length in nanometers. Interactions are not calculated between atoms bonded to each other (1,2 interactions) or atoms involved in angle interactions (1,3 interactions). In addition, van der Waals interactions are calculated only for pairs of atoms within a cutoff distance of 0.9 nm. To avoid discontinuous forces, Eq. (5) is multiplied by a switching function. The Dreiding force field assumes the standard combination rules:

$$x_{ij} = \mathrm{RE}_i + \mathrm{RE}_j$$
$$D_{ij} = (\mathrm{DE}_i \times \mathrm{DE}_j)^{1/2},$$

where RE is the atomic van der Waals radius in nanometers, and DE is the atomic van der Waals energy in kilojoules per mole.

The van der Waals radius and well depth for hydrogen was determined by ab initio calculations on the molecular hydrogen dimer.

Electrostatic interactions are calculated by:

$$E_{el} = (33.20647)Q_iQ_j/\varepsilon R_{ij}. \qquad (6)$$

Q_i and Q_j are charges in electron units, R_{ij} is the distance in nanometers, and ε is the dielectric constant. Interactions are not calculated between atoms bonded to each other (1,2 interactions) or those involved in angle

interactions (1,3 interactions). Electrostatic interactions are calculated only for pairs of atoms within a cutoff distance of 0.9 nm. Equation (6) is modified by a switching function.

An explicit hydrogen-bonding potential is employed by the Dreiding force field,

$$E_{hb} = D_{hb}\{5[R_0/R]^{12} - 6[R_0/R]^{10}\}\cos^4(\theta_{AHD}), \quad (7)$$

where D_{hb} is the hydrogen-bond strength in kilojoules per mole, R_0 is the natural distance between the acceptor and donor atoms in nanometers, and θ_{AHD} is the bond angle between the hydrogen acceptor and the hydrogen donor. Hydrogen-bonding interactions are calculated only for pairs of atoms within a cutoff distance of 0.9 nm. The only atoms allowed to take part in hydrogen bonding are oxygen, nitrogen, sulfur, fluorine, and chlorine. Equation (7) is modified by both distance and angular switching functions.

D_{hb}, the hydrogen-bond energy, is set to -39.8 kJ, independent of donor and acceptor, and R_0, the bond distance between acceptor and donor atoms, is set equal to 0.275 nm for all hydrogen bonds involving oxygen, nitrogen, sulfur, fluorine, and chlorine.

The coordinates of atoms in ZSM-5, benzene, toluene, and xylenes were computed by the graphic supercomputer TITAN 3000 (Srardent Inc.) applying the PolyGraf software offered by BioDesign Inc. The coordinates of ZSM-5 were computed with the values cited in Kokotailo *et al.* (*10*).

The initial position of these aromatic molecules stayed on a line extending from the ZSM-5 pore channel center.

While these molecules approached and diffused inside the pores of ZSM-5, the energy calculations for the force field were conducted to energy 0.05-nm interval on 1152 atoms of ZSM-5, which corresponds to the pore length of 5 nm, and on an organic molecule. The energy minimizations were followed by short dynamic runs (0.1 ps, 600 K) applying the conjugate gradient minimization scheme and then reminimized. The computational time was extremely shortened by means of vector/parallel optimization. Moreover, to increase the precision,

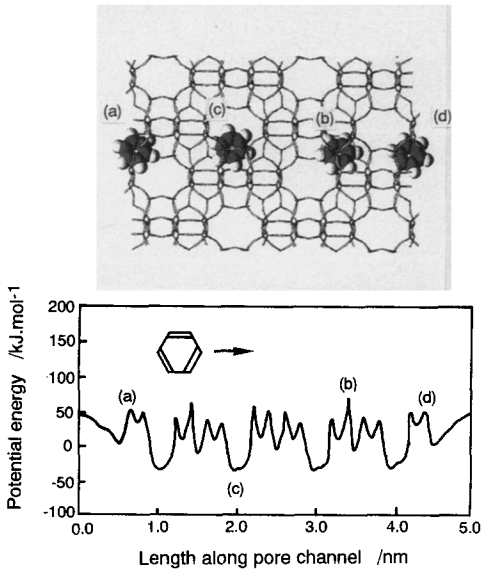

FIG. 2. The potential energy for driving molecule along the pore channel of ZSM-5 and its visualization with the aid of computer graphics. Position of molecule: (a) entrance of the pore channel, (b) the highest-energy level, (c) the lowest-energy level, (d) exit of the pore channel. The kind of molecule and the entering direction of molecule designated by arrow mark are shown with each part.

FIG. 2.1. Solid line, benzene.

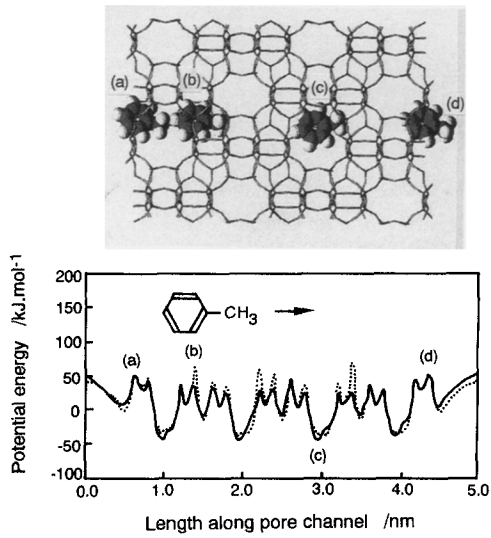

FIG. 2.2 Solid line, toluene; dotted line, benzene.

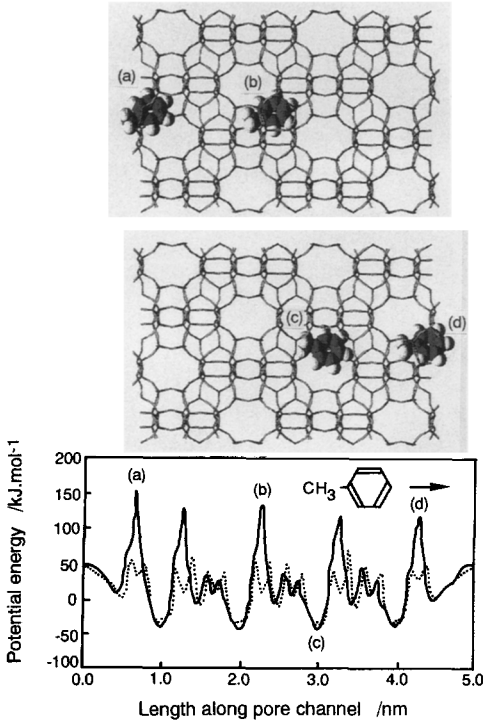

FIG. 2.3 Solid line, toluene; dotted line, benzene.

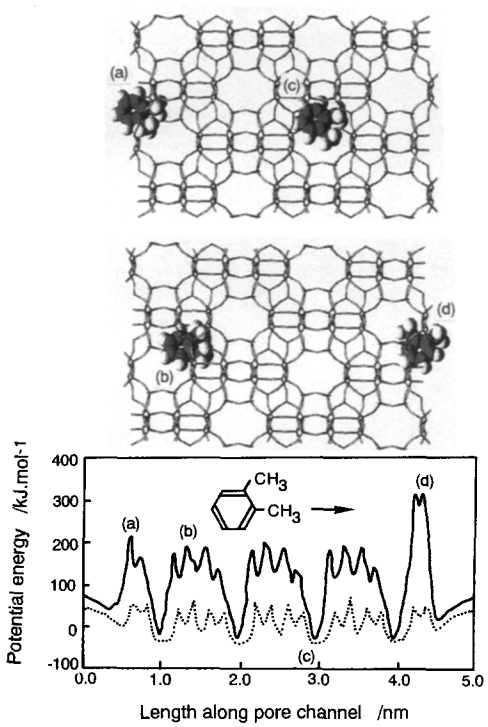

FIG. 2.4. Solid line, *o*-xylene; dotted line, benzene.

the interactions between molecules and large crystals were calculated applying periodic boundary conditioning.

For the display of space-filling models of the aromatic hydrocarbons and ZSM-5, the radius of van der Waals and ion radius by Pauling were used, respectively.

RESULTS AND DISCUSSION

The display of the crystal structure of ZSM-5 by computer graphics is shown in Fig. 1. Large spheres and small ones show oxygen atoms and silicon atoms, respectively. Four oxygen ions around a Si ion are coordinated at the corners of a regular tetrahedron. These units are coupled, then make the ring of 10 oxygen atoms, obeying the pentasil structure.

Energy variations of these aromatic molecules, which enter the pores of ZSM-5 from different positions of the molecules and pass through the pore channel of 5 nm length, are shown in Figs. 2.1 to 2.8. In these figures, the position of the guest molecule refers to the center of mass. The energy calculation is visualized by the aid of computer graphics and superimposed in each figure.

The results of energy calculation for the force field while benzene approaches and diffuses inside the pores of ZSM-5 are shown in Fig. 2.1. The energy level of benzene decreased with an approach to the pore opening of ZSM-5. Although the size of the benzene molecule is barely larger than the diameter of a 10-oxygen member ring of ZSM-5 by computer graphic display, it is clear that the benzene molecule is twisted to enter the pores of ZSM-5. From the energy calculation of the force field, it can be seen that the energy level of benzene excited was increased to 52.8 kJ · mol^{-1} at the pore entrance of ZSM-5.

During the diffusion process of benzene through the pores of ZSM-5, benzene had the lowest energy level, −36.4 kJ · mol^{-1}

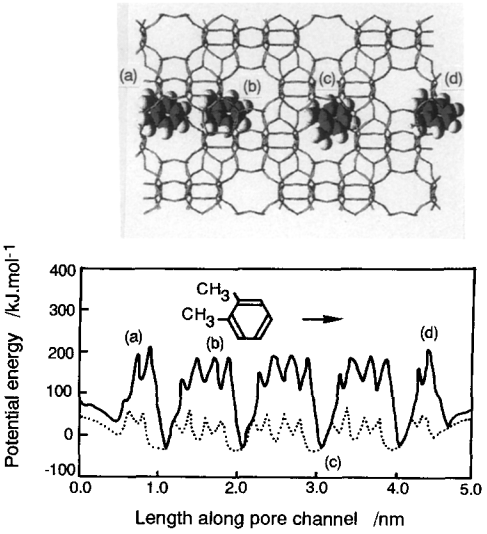

FIG. 2.5. Solid line, *o*-xylene; dotted line, benzene.

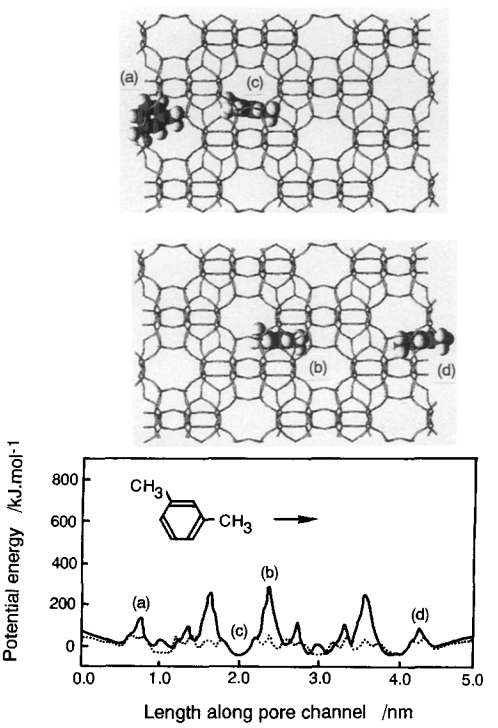

FIG. 2.6 Solid line, *m*-xylene; dotted line, benzene.

at the position of intersectional parts of pores. On the other hand, benzene at the position of the pore entrance had the highest energy level. The display of computer graphics shows the diffusion states of benzene while rolling.

Figures 2.2 and 2.3 show the states of toluene molecules entering into the pores of ZSM-5 from the methyl group and from the 4-position, respectively, and passing through the pore channel. In Fig. 2.2, the toluene molecule approaches and diffuses inside the pores of ZSM-5 with the methyl group in front. The energy level of toluene decreases with an approach to ZSM-5, which is similar to that of benzene. However, except for the position of the pore exit, both the maximum and the minimum potential energies of toluene seem to be lowered at exactly the same positions where benzene has maximum and minimum potential energy, respectively. The reason for this difference is considered to be that from the comparison between computer graphics of Figs. 2.1 and 2.2, the existence of the methyl group plays a role in decrease in molecule pitching.

On the other hand, Fig. 2.3 shows that the maximum energy level of toluene faced with the carbon at the 4-position of toluene to the pore of ZSM-5 was 153 kJ · mol^{-1}. That was much larger than in the case of Fig. 2.2. From a comparison of computer graphics between Figs. 2.2 and 2.3, it can be seen that the large potential energy corresponds to the stronger rolling of the molecule. Computer graphics at this position show that the methyl group is caught by the intersectional parts of the pore channels, and then the molecule continues along the pore, rotating in the direction of the benzene-ring plane.

Energy variation of xylenes, which enter the pores of ZSM-5 with different molecule positions in front and pass through the pore channels of 5 nm length, are shown in Figs. 2.4 to 2.8.

Figures 2.4 and 2.5 show the states of *o*-xylene molecules entering into the pores of ZSM-5 with the methyl group and with the 4-position in front, respectively, and passing through the pore channels. Both figures are very similar to each other except around the pore exits in Fig. 2.4. The

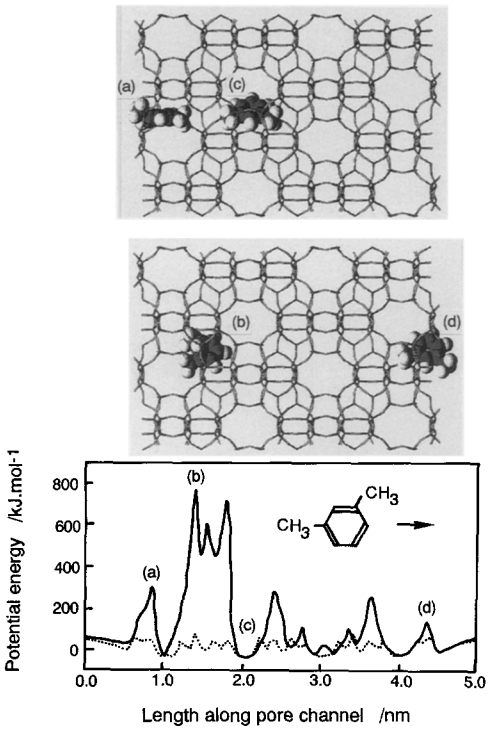

FIG. 2.7 Solid line, *m*-xylene; dotted line, benzene.

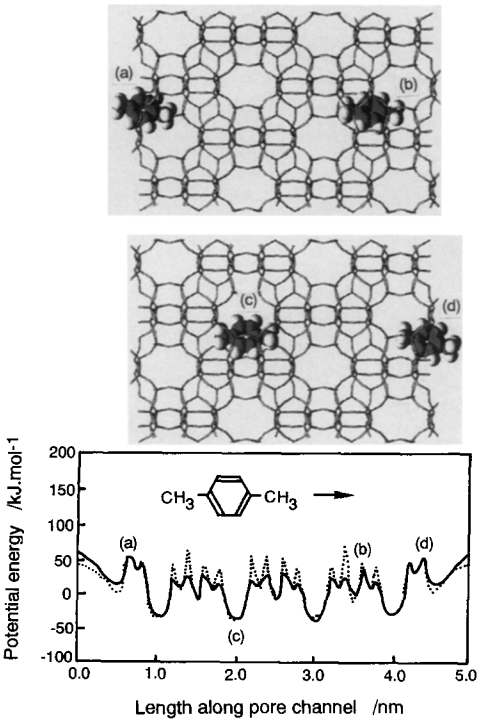

FIG. 2.8 Solid line, *p*-xylene; dotted line, benzene.

potential energy for this exception shows the highest level. The computer graphics at this position show that the methyl group of the *ortho*-position is caught by the pore exits, and then the molecule moves out while rotating in the direction of the benzene-ring plane, and as a result, the molecule leaves from the pores in the same direction as Fig. 2.5.

The results of *m*-xylenes approaching the pore entrances with the methyl group and with the 4-position in front are shown in Figs. 2.6 and 2.7, respectively. From the comparison between Figs. 2.6 and 2.7, it can be seen that the energy level of *m*-xylene is much lower than that of *o*-xylene and often it approaches the same lower level of benzene, although at the same parts of the channel the peak of energy reaches the same level as that of *o*-xylene. Figure 2.6 shows that when *m*-xylene enters with the 4-position in front, it advances to 1.3 nm with rolling by 90°, and at this point the energy level increases to a very high level, 795 kJ · mol^{-1}. This position is an intersectional part of pores. The methyl group of the *meta*-position is caught in this intersectional part, and the *m*-xylene molecule rotates about 60° in the direction of the benzene-ring plane. After that, the *m*-xylene molecule advances with the methyl group of the *meta*-position in front, the same way as in Fig. 2.6, and consequently, the variations of energy coincide with each other.

In the case of *p*-xylene, only the direction of entering with the methyl group in front should be considered, and the results are shown in Fig. 2.8. The other direction of *p*-xylene entering into the pore opening is too difficult owing to the hindrance of two methyl groups. It is noteworthy that two methyl groups of *p*-xylene rotate like a propeller and stabilize the pitching and rolling of the benzene plane. These features reflect the decrease in energy levels at peak positions for the benzene molecules.

From the calculation results and the

TABLE 1

Calculation Results of Energy Levels of the Aromatic Hydrocarbons Studied inside the Pores of ZSM-5

Aromatics	At the entrance of pore ($kJ \cdot mol^{-1}$)	At the exit of pore ($kJ \cdot mol^{-1}$)	At the inside of pore	
			Highest ($kJ \cdot mol^{-1}$)	Lowest ($kJ \cdot mol^{-1}$)
Benzene	52.8	49.4	68.2	−36.4
Toluene[a]	153	118	132	−44.0
Toluene[b]	50.2	55.7	36.0	−44.4
o-Xylene[a]	214	210	191	−27.6
o-Xylene[b]	215	324	193	−29.3
m-Xylene[a]	306	145	775	−36.4
m-Xylene[b]	147	103	293	−40.2
p-Xylene	56.1	53.6	33.5	−37.7

[a] Passes through the channel of ZSM-5 from the 4-position in front.
[b] Passes through the channel of ZSM-5 from the methyl carbon in front.

computer graphics of xylene isomers, *p*-xylene is most stable among xylene isomers. *meta*-Xylene is more stable than *o*-xylene.

The diffusion of toluene and xylenes molecules inside the pores of ZSM-5 faced with the methyl group is comparatively stable. When *o*- and *m*-xylene molecules approach the pores of ZSM-5 with the 4-position in front, they rotate during the diffusion process inside the pore channels, then pass through the channel with the methyl group in front. At high-energy level places, where diffusion resistances are quite large, these molecules cause rolling and pitching inside the pores of ZSM-5.

The energy values obtained by the force field calculation for benzene, toluene, and xylenes at distinct positions are summarized in Table 1.

In conclusion, distinct differences of the potential energy of molecules induced by their microscopic situation in the domain of zeolite pores were described by both energy calculations for force fields and computer graphics, complementary to each other. Dynamic behaviors of molecules must be made more realistic by adding the factor of vibration of zeolite lattice. The simulation and visualization of dynamic behaviors of molecules, such as performed in this study, will facilitate investigation of the adsorption and catalysts on microporous crystals.

REFERENCES

1. Jacobs, P. A., and van Santen, R. A., Eds., "Zeolites: Facts, Figures, Future," Parts A and B. Elsevier, Amsterdam, 1989.
2. Inui, T., Makino, Y., Okazumi, F., Nagano, S., and Miyamoto, A., *Ind. Eng. Chem. Res.* **26,** 647 (1987).
3. Inui, T., Miyamoto, A., Matsuda, H., Nagata, H., Makino, Y., Fukuda, K., and Okazumi, F., *in* "Proceedings, 7th Zeolite Conf., Tokyo" (Y. Murakami, A. Iijima, and J. W. Ward, Eds.), p. 859. Kodansha-Elsevier, Tokyo, 1986.
4. Derouane, E. G., "Intercalation Chemistry," p. 101. Academic Press, New York, 1982.
5. Nowak, A. K., Cheetham, A. K., Picket, S. D., and Ramdas, S., *Mol. Simulation* **1,** 67 (1987).
6. Mentzen, B. F., and Bosselet, F., *CR Acad. Paris* **309**(2), 539 (1989).
7. Inui, T., and Nakazaki, Y., *Zeolites* **11,** 434 (1991).
8. Dasgupta, S., and Goddard, W. A., III, *J. Phys. Chem.* **90,** 7207 (1989).
9. Mayo, S. L., Olafson, B. D., and Goddard, W. A., III, *J. Phys. Chem.* **94,** 8897 (1990).
10. Kokotailo, D. T., Lawton, S. L., Olson, D. H., and Meier, W. M., *Nature* **272,** 437 (1978).